Maps of structured aerosol activity during the MY 25 planet-encircling dust storm on Mars

John Noble[1,2], R. John Wilson[3], Bruce A. Cantor[4], Jeffrey R. Barnes[5]
Melinda A. Kahre[1], Jeffery L. Hollingsworth[1], Alison F. C. Bridger[1,2], Robert M. Haberle[1]

1. NASA/Ames Research Center, 2. San José State University, 3. NOAA Geophysical Fluid Dynamics Laboratory, 4. Malin Space Science Systems, 5. Oregon State University

Introduction

We present 42 maps of the areal extent of structured dust activity from L_s=165.1–187.7°, MY 25. The primary motivation of this work is to examine the temporal and spatial relationship between dust storms observed by the Mars Orbiter Camera (MOC) and baroclinic eddies inferred from Fast Fourier Synoptic Mapping (FFSM) of TES temperatures (Barnes 2001, 2003, 2006). Previous investigation into this relationship has yielded important clues to the role eddies may play in dust storm initiation (Noble 2013; Noble *et al.* 2011). The maps presented here are used to determine the distribution and evolution of dust storms for this analysis.

A secondary motivation is to provide improved input to Mars general circulation model (MGCM) simulations (Noble *et al.* 2008; Wilson *et al.* 2008). Significant portions of the TES dust opacity retrievals are missing or unreliable due to diminished contrast and extreme opacity levels. TES opacity retrieval reliability is partially a function of ground-air temperature contrast, with reliability diminishing as contrast approaches zero. Contrast limits occur at high-latitudes (>55° N, <60° S) and in extremely dusty conditions. These data gaps often occur in important times and places (*e.g.* Hellas and Claritas) during storm initiation and expansion, and likely decrease the reliability of MGCM simulations forced with TES dust (Wilson 2016).

The time domain of this investigation, L_s=165.1–187.7°, was chosen to match corresponding FFSM data. This time series starts 21 sols before the precursor phase and ends on the fifth sol of the expansion phase. The primary region of interest (ROI) is the Hellas quadrant where PDS initiation began, and the secondary ROI is the southern hemisphere (30–60° S) where eddy activity is strongest. Structured dust activity throughout the southern hemisphere was mapped, along with most major storms in the northern hemisphere.

TES FFSM eddies & MOC dust storms (50-55° S), 3.7 hPa, 55° S, MY 25, L_s=165.1-187.7°

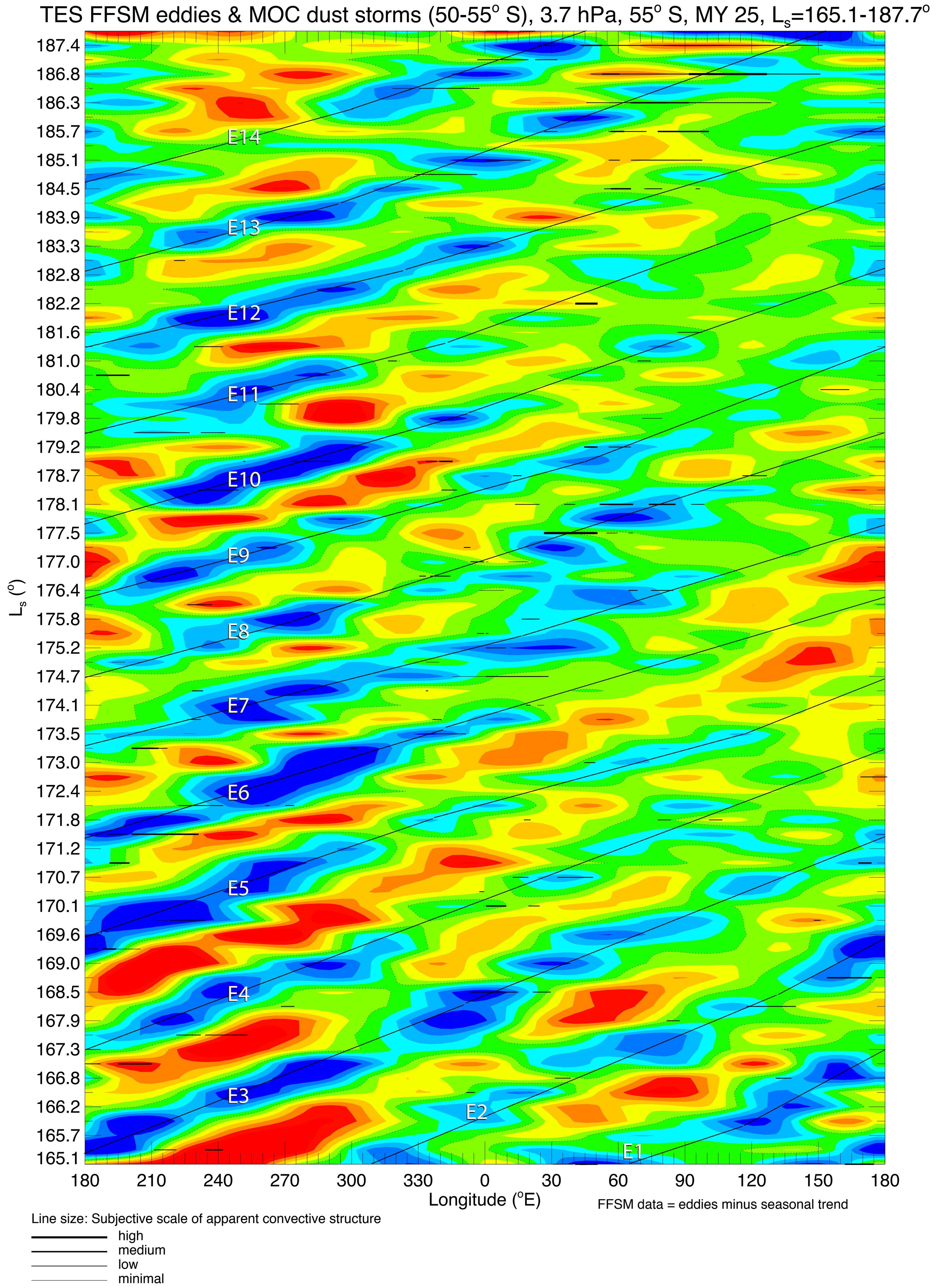

Eddy # 8

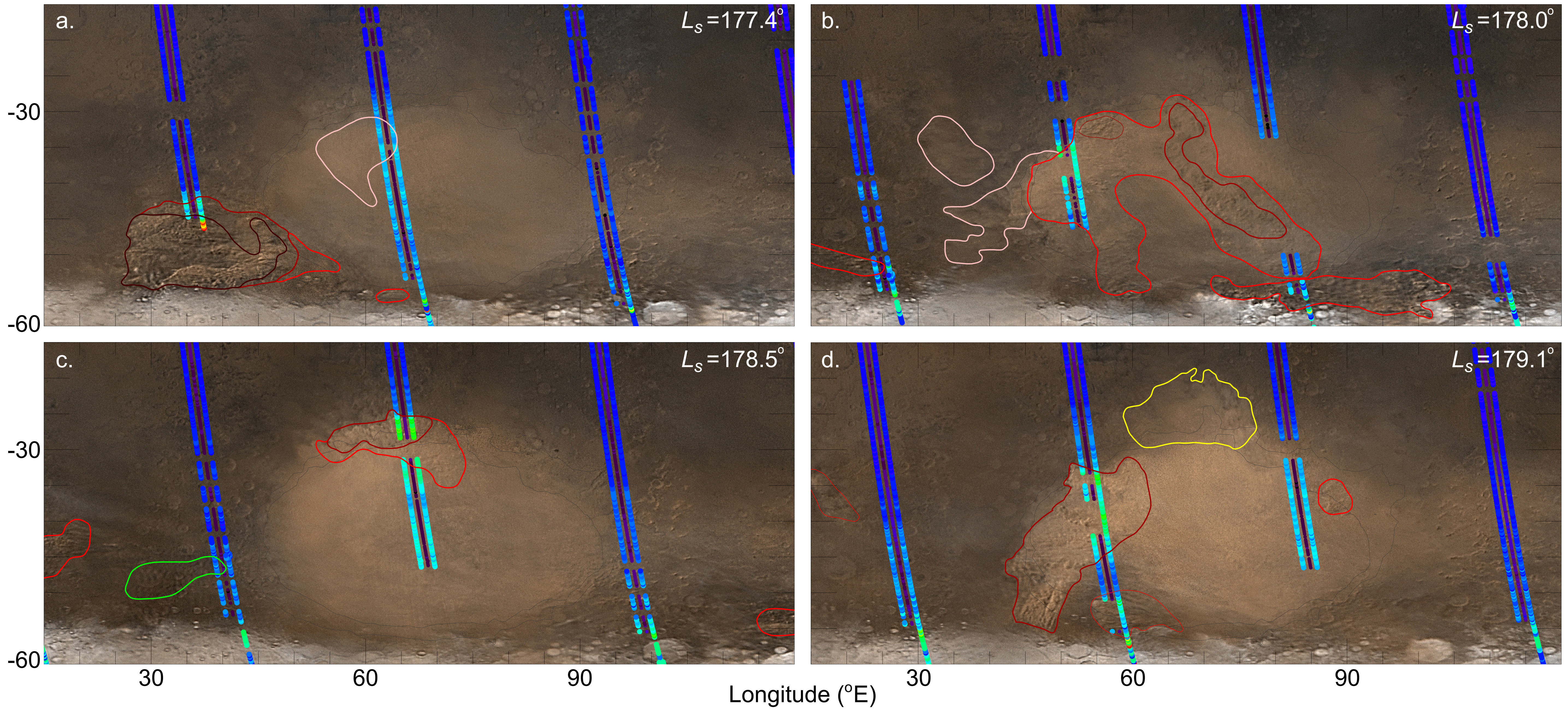

Eddy # 11

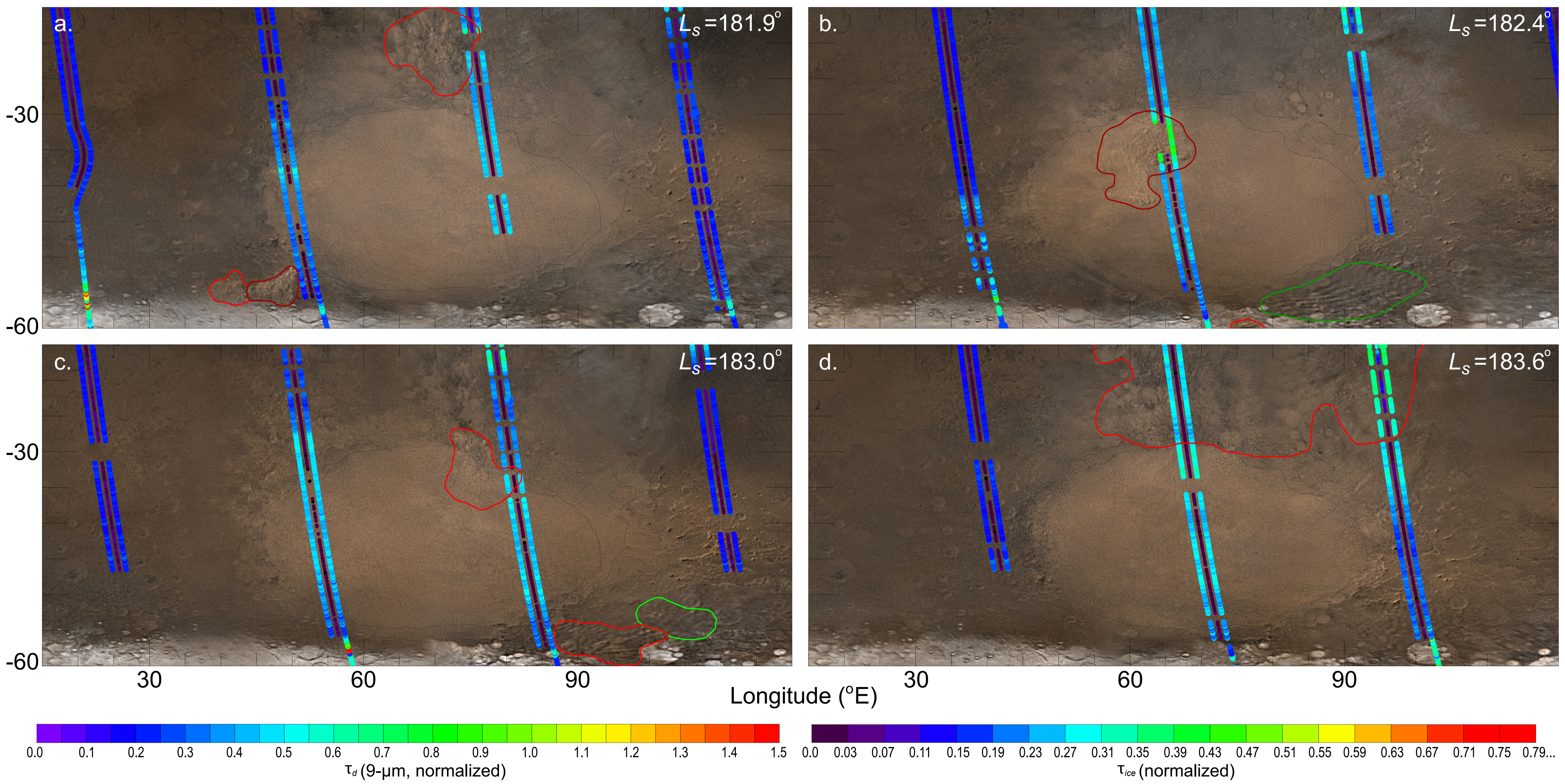

MOC daily global maps courtesy of Malin Space Science Systems

Structured aerosol activity classification scheme

We created a classification scheme of structured aerosol activity based on subjective visual interpretation of MOC imagery. Three dust activity categories were represented: dust storms; dust clouds; and ripple patterns. Dust storms represent our interpretation of dust activity over source regions. Dust clouds represent our interpretation of dust activity over non-source regions. Ripple patterns have a rippled or washboard-like structure with parallel linear bands and appear to contain dust. Some or all of these occurrences may be dust entrained in lee wave clouds.

	Aerosol activity			Dust storm & dust cloud
Structure	Dust storms	Dust clouds	Ripple patterns	Description & features
3	113	213	313	Structure = high • large lobes and plumes • strong shadows & contrast
2	112	212	312	Structure = medium • medium lobes and plumes • medium shadows & contrast
1	111	211	311	Structure = low • small lobes; small plumes in craters • weak shadows & contrast
0	110	210	N/A	Structure = none/minimal • no lobate features • no/minimal shadows & contrast

Phase speed and periodicity

Assuming that the eddies were globally coherent, we calculated their phase speed, c, using: $c(x) = \Delta x/\Delta t$, where $\Delta x = (r_{eq} \cdot \cos\varphi) \cdot \Delta\lambda$, r_{eq} is planetary radius, φ is latitude, λ is longitude, and t is time at 45° E. Storm migration speed was calculated in the sector between Argyre and Eastern Promethei (~330–140° E).

Integration and analysis of FFSM and MOC data show concurrent eastward migration of eddies and dust storms in the Hellas quadrant.

Eddy #	Eddy period (*P*) @ 45° E (sols)	Eddy phase speed (*c*) global (m/s)	Storm migration speed (~330–140° E) Argyre → Promethei (m/s)
1	—	—	11.9
2	4.2	13.3	12.0
3	3.3	14.6	13.0
4	3.0	16.1	11.7
5	3.2	15.9	—
6	2.4	17.7	—
7	3.1	16.2	13.0
8	2.3	16.8	15.0
9	3.1	16.0	11.1
10	2.8	15.5	15.7
11	2.7	15.2	10.3
12	3.4	—	—
13	3.0	—	13.4
14	—	—	—

Summary

This work has two implications for martian atmospheric science. First, integration of MGS data has enabled us to develop improved quantitative and qualitative descriptions of storm evolution that may be used to constrain estimates of dust lifting regions, horizontal dust distribution, and to infer associated circulations. Second, we believe that these maps provide better bases and constraints for modeling storm initiation (Noble *et al.* 2008; Wilson *et al.* 2008). Assuming that structured dust storms indicate active dust lifting (Guzewich *et al.* 2015; Noble *et al.* 2010), these maps allow us to define potential dust lifting regions. Furthermore, these maps provide a scale of potential lifting regions that can be included or excluded in simulations, assuming that greater degrees of visible structure indicate more vigorous lifting. We are continuing to refine these maps and use them as input to MGCM simulations.

Working Hypothesis

Based on our analysis of these MGS data, we propose the following working hypothesis to explain the dynamical processes responsible for PDS initiation and expansion. Six eastward-traveling transient baroclinic eddies triggered the MY 25 precursor storms in Hellas during L_s=176.2–184.6° due to the enhanced dust lifting associated with their low-level wind and stress fields. This was followed by a seventh eddy that contributed to expansion on L_s=186.3°. Increased opacity and temperatures from dust lifting associated with the first three eddies enhanced thermal tides which supported further storm initiation and expansion out of Hellas. Constructive interference of eddies and other circulation components including sublimation flow, anabatic winds (daytime upslope), and diurnal tides may have contributed to storm onset in, and expansion out of Hellas. Non-dynamical factors in PDS interannual variability include dust sources and sinks

References

Cantor, B. A., 2007: MOC observations of the 2001 Mars planet-encircling dust storm. *Icarus* , 186, 60-96

Noble, J., R. M. Haberle, A. F. C. Bridger, J. Wilson, J. R. Barnes, J. Murphy, J. Hollingsworth, M. C. Malin, B. A. Cantor, M. Smith, and T. Martin, 2007: Integration of MGS Observations of the 2001 Global Dust Storm on Mars: Implications for Atmospheric Modeling. *AGU Fall Meeting* , San Francisco, CA, USA, American Geophysical Union.

Noble, J., R. J. Wilson, R. M. Haberle, J. L. Hollingsworth, M. A. Kahre, J. R. Barnes, A. F. C. Bridger, and B. A. Cantor, 2011: Comparison of TES FFSM Eddies and MOC Storms, MY 24-26. *Fourth International Workshop on the Mars Atmosphere: Modelling and observations* , Paris, France, CNES, ESA, NASA

Wilson, R. J., R. M. Haberle, J. Noble, A . F. C. Bridger, J. Schaeffer, J. Barnes, and B. Cantor, 2008: Simulation of the 2001 planet-encircling dust storm with the NASA/NOAA Mars general circulation model. *Third International Workshop on the Mars Atmosphere: Modeling and Observations* , Williamsburg, VA, USA.

Wilson, R. J., J. Noble, and S. J. Greybush, 2011: The derivation of atmospheric opacity from surface temperature observations. *Fourth International Workshop on the Mars Atmosphere: Modelling and Observations* , Paris, France.